Electronic Supplementary Material (ESI) for ChemComm.
This journal is © The Royal Society of Chemistry 2022

Supporting Information

$Pd_{17}Se_{15}$ alloy on Se sphere with high anti-poisoning ability for alcohol fuel oxidation

Wei Qiao[a], Meng Zha[a,c], Yun Yang[*b], Guangzhi Hu[c], Ligang Feng[*a]

a School of Chemistry and Chemical Engineering, Yangzhou University, Yangzhou, 225002, PR China.

b Nanomaterials and Chemistry Key Laboratory, Wenzhou University, Wenzhou, China. bachier@163.com.

c School of Chemical Science and Engineering, School of Energy, Yunnan University, Kunming 650091, China

Experiments

Materials and chemicals

Chemicals

All the reagents in the experiment were analytical grade and used as received. Selenium dioxide (SeO_2), glucose ($C_6H_{12}O_6$), palladium chloride ($PdCl_2$), ethylene glycol ($C_2H_6O_2$), L-ascorbic acid were purchased from Shanghai Aladdin Bio-Chem Technology Co., Ltd. KOH were purchased from Sinopharm Chemical Reagent Co., Ltd. Nafion (5 wt.%) was purchased from Sigma-Aldrich. Commercial Pd/C (20 wt.% Pd) catalyst was bought from Alfa Aesar (Tianjin) Chemical Co., Ltd. All solutions were prepared with ultrapure water by Lab Water Purification System (Thermo Fisher Scientific (USA) Co., Ltd).

Synthesis of Se spheres

First, 0.18 g of SeO_2 and 1.5 g of glucose were added to a beaker and dissolved in 15 mL of ultrapure water under vigorous magnetic stirring at room temperature to form a homogeneous solution. Then the solution was transferred into the Teflon-lined stainless steel with a volume capacity of 25 mL, sealed and reacted at 200 ^{o}C for 6 h. The product was filtered to obtain the black precipitate. Finally, the precipitate was washed three times with anhydrous ethanol and ultrapure water and then dried overnight in a vacuum at 60 ^{o}C to get the Se microspheres.

Synthesis of $Pd_{17}Se_{15}$/Se catalyst

40 mg of Se microspheres obtained above were ultrasonically dispersed in an in-situ flask containing 100 mL ethylene glycol to form a uniform suspension. A certain

amount of $PdCl_2$ solution (containing 27 mg Pd) was added to the suspension under stirring. After mixed well, the suspension was placed and exposed in the middle of a microwave oven with 700 W with 60 s for 3 times and cooled to room temperature naturally. At last, the suspension was filtered, washed and dried overnight at 60 ^oC in a vacuum oven to obtain $Pd_{17}Se_{15}$/Se catalyst.

Physical Characterizations

The catalysts were characterized by Bruker D8 advance X-ray diffraction (XRD) with Cu Kα radiation. X-ray photoelectron spectroscopy (XPS) measurement was carried on an ECSALAB250Xi S3 spectrometer with an Al Kα radiation source. The morphology and microstructure of the product were analyzed by scanning electron microscopy (FESEM, Hitachi, S-4800 II, Japan) and transmission electron microscopy (TEM, Philips, TECNAI 12, Holland). High-resolution transmission electron microscopy (HRTEM) was performed on a FEI TECNAI G2 F30 STWIN (USA) operating at 300 kV. The element mapping analysis and energy-dispersive X-ray detector spectrum (EDX) images were obtained on a TECNAI G2 transmission electron microscope equipped with an EDXA detector: the microscope was operated at an acceleration voltage of 200 kV.

Electrochemical Measurements

All electrochemical measurements were performed using a bio-logic VSP electrochemical workstation (bio-logic Co., France) and a conventional three-electrode system. The working electrode was a glassy carbon electrode (diameter 3 mm, 0.07 cm^{-2}). The graphite rods and saturated calomel electrodes (SCE, Hg/Hg_2Cl_2) were used as

a counter and a reference electrode by a double-salt bridge with single-tube capillary tips, and the potential was carefully checked before and after measurement. The $Pd_{17}Se_{15}$/Se catalyst ink was a mixture of 2 mg of catalyst, 3 mg of carbon black, 950 μL of ethanol, and 50 μL of a 5 wt. % Nafion solution dispersed by ultrasound. The Pd catalyst ink containing 1 mg catalyst and 4 mg carbon black, and were prepared the same component ink solution of 1000 μL. Next, 5 μL of the catalyst ink was pipetted onto a pre-cleaned working electrode and let the ink dry naturally. The loading of Pd on the electrode was 0.03 mg cm^{-2}.

Cyclic Voltammetry Measurements

The electrolyte was firstly bubbled with high purity nitrogen for 15 minutes to remove the dissolved oxygen. The methanol oxidation experiment was conducted in an electrolyte of a mixed solution of 1.0 M KOH and 1.0 M CH_3OH at a potential range between -1.0 V and 0.2 V vs. SCE at a potential scan rate of 50 mV s^{-1}. The oxidation of ethanol was measured in an alkaline solution carried out at room temperature in 1.0 M KOH and 1.0 M CH_3CH_2OH solution at a potential range between -1.0 V and 0.2 V vs. SCE at a potential scan rate of 50 mV s^{-1}.

CO stripping measurements

The high purity CO (99.9%) was bubbled to the electrolyte 1.0 M KOH for 15 minutes when the potential was controlled at -0.8 V vs. SCE. Then the nitrogen was bubbled into the electrolyte for 15 min to remove the excess CO dissolved in the electrolyte. The potential range of CO stripping was -1 ~ 0.2 V vs. SCE at a potential

scan rate of 20 mV s^{-1}. The electrochemical active surface areas (ECSA) were estimated based on the following formula:

$ECSA = Q/Sl.$

Where Q is calculated by integrating the charges associated with the PdO reduction peak; l is the loading of Pd on the surface of the electrode (in mg) and S is a proportionality constant of 405 μC·cm^{-2}.[1]

Chronoamperometry measurements

To evaluate the stability of the alkaline methanol oxidation catalyst, the chronoamperometry (CA) experiment was carried out in 1 M KOH and 1.0 M CH_3OH solutions at -0.25 V vs. SCE for methanol oxidation. And the CA experiment of the alkaline ethanol oxidation catalyst was carried out in 1 M KOH and 1 M CH_3CH_2OH solutions at -0.25 V vs. SCE.

Electrochemical Impedance Measurements

The electrochemical impedance spectra (EIS) were recorded at the frequency range from 1000 kHz to 30 mHz. The amplitude of the sinusoidal potential signal was 5 mV.

Computational methods

The CASTEP module of the Materials Studio software (Accelrys Inc.) was employed for thequantum chemistry calculations. Perdew−Burke−Ernzerh (PBE) of approximation was selected as the generalized gradient approximation (GGA) method to calculate the exchange-correlation energy. The Broyden−Fletcher−Goldfarb−Shanno (BFGS) scheme was selected as the

minimization algorithm. And DFT-D correction was used for dispersion corrections. Hubbard U-corrections to the delectrons of V (LDA+U, effective U(V) = 2.5 eV) and spin-polarized were performed during the calculations. The energy cut off is 380 eV and the SCF tolerance is 1.0×10^{-6} eV/atom. The optimization is completed when the energy, maximum force, maximum stress and maximum displacement are smaller than 5.0×10^{-6} eV/atom, 0.01 eV/Å, 0.02 GPa and 5.0×10^{-4} Å, respectively. A vacuum slab exceeding 15 Å was employed in the z direction to avoid the interaction between two periodic units. The surface model consists of the (001) surface of $Pd_{17}Se_{15}$ alloy placed on the stoichiometric surface, and CO is adsorbed on the Pd site on the (001) surface of $Pd_{17}Se_{15}$ alloy.[2] The (110) surface of Pd adopts a double-layer structure, and CO is adsorbed at the vertex of the (110) surface of Pd. The adsorption energy (E_{ads}) between the surface and adsorbed particles was computed by eqs(1),(2).[3]

$$E_{ads1} = E_{Pd_{17}Se_{15}\text{-}CO} - E_{CO} - E_{Pd_{17}Se_{15}} \quad (1)$$

$$E_{ads2} = E_{Pd\text{-}CO} - E_{CO} - E_{Pd} \quad (2)$$

where $E_{Pd_{17}Se_{15}\text{-}CO}$ and $E_{Pd\text{-}CO}$ is the total energy of the system after adsorbing the molecule, E_{CO} is the energy of adsorption molecules, and $E_{Pd_{17}Se_{15}}$ and E_{Pd} is the total energy of the system before adsorbing the molecule.

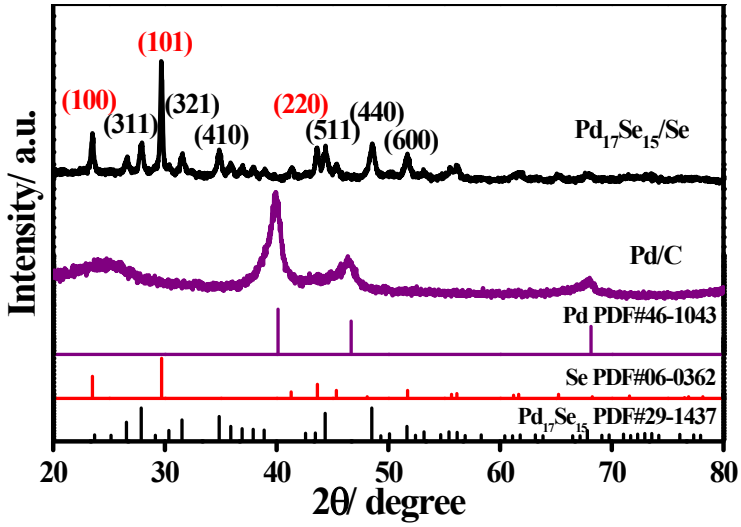

Fig. S1 XRD patterns of $Pd_{17}Se_{15}$/Se and Pd/C catalysts.

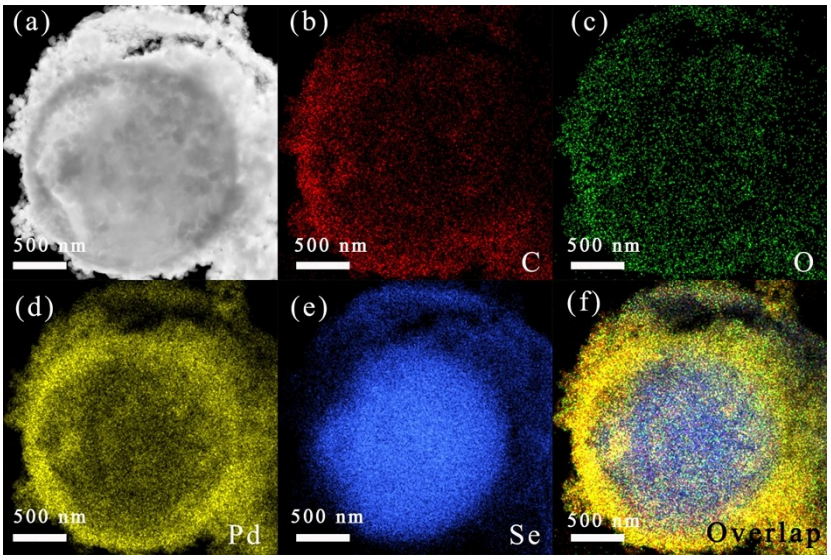

Fig. S2 STEM and elemental mapping images of $Pd_{17}Se_{15}$/Se catalyst.

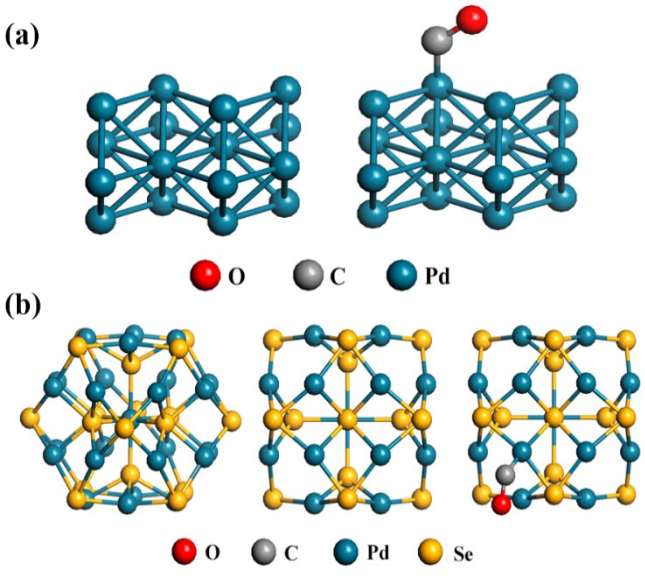

Fig. S3 (a) Model of Pd metal before and after CO adsorption; (b) Model of $Pd_{17}Se_{15}$ and top view before and after CO adsorption.

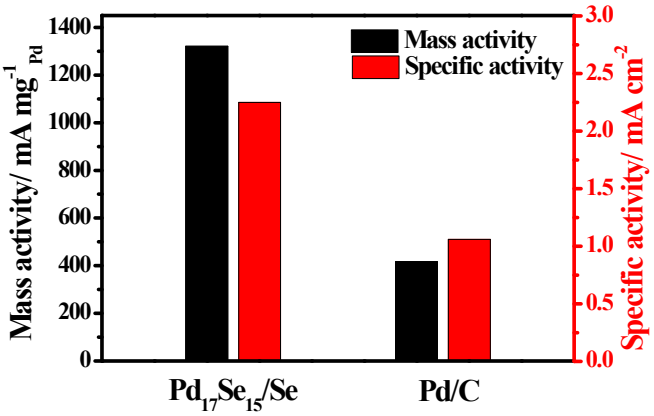

Fig. S4 Graphical comparison of mass and specific activity of $Pd_{17}Se_{15}$/Se and Pd/C catalysts for methanol oxidation in the 1 M KOH + 1 M CH_3OH solution.

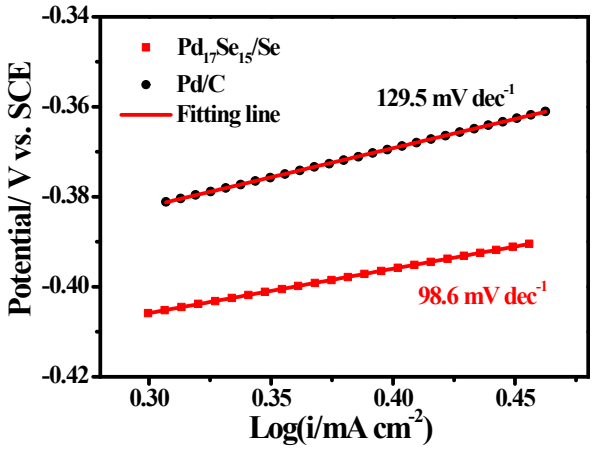

Fig. S5 Tafel plots of $Pd_{17}Se_{15}$/Se and Pd/C catalysts for methanol oxidation.

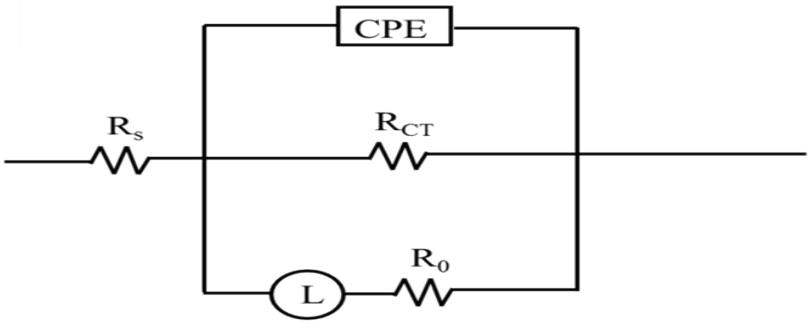

Fig. S6 Equivalent circuit for EIS analysis in the 1 M KOH + 1 M CH_3OH solution. For equivalent circuits, R_s represents uncompensated solution resistance; R_{ct} corresponds to charge transfer resistance generated by alcohol oxidation. R_0 may be related to the contact resistance between catalyst material and glassy carbon electrode; the constant phase element (CPE) composition is for double-layer capacitance; and the L usually comes from the external circuit inductance and usually does not involve an electrochemical process.

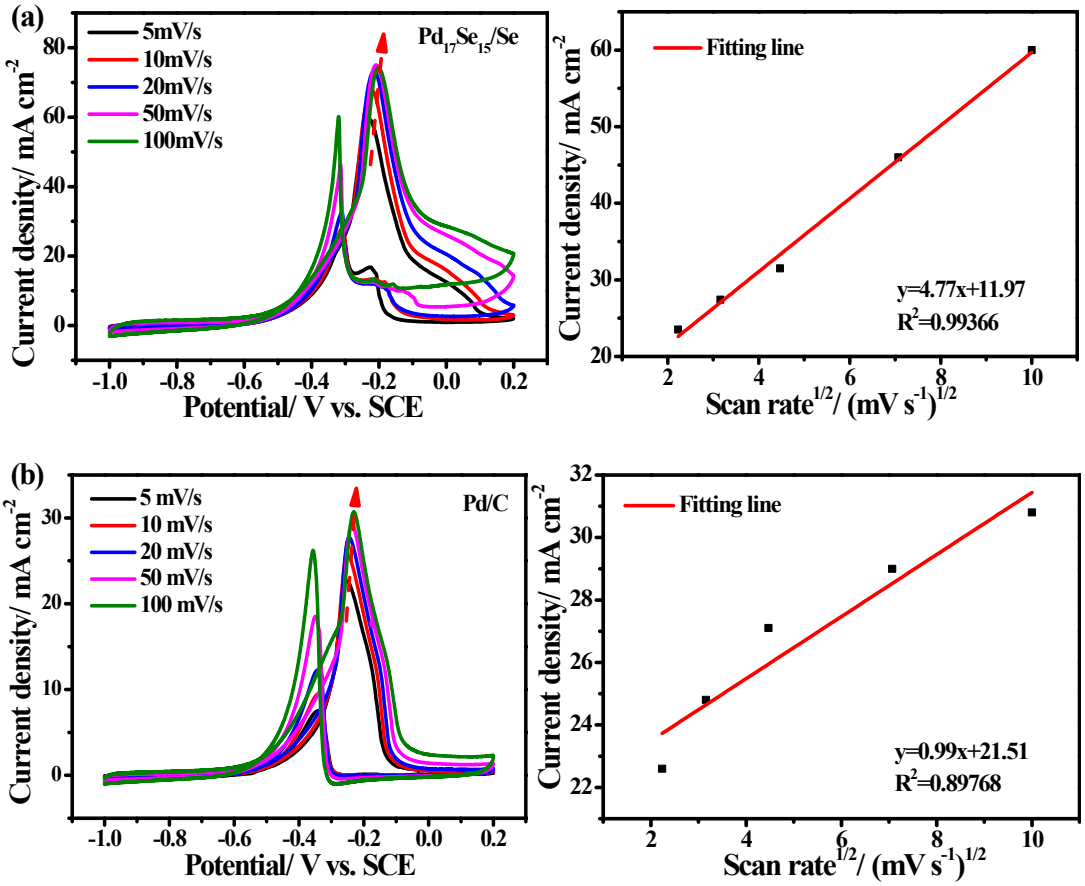

Fig. S7 Cyclic voltammograms of the $Pd_{17}Se_{15}$/Se (a) and Pd/C (b) catalysts in 1 M KOH + 1 M CH_3OH at scan rates of 5, 10, 20, 50, 100 mV s^{-1} and corresponding peak current density versus the square root of the scan rates.

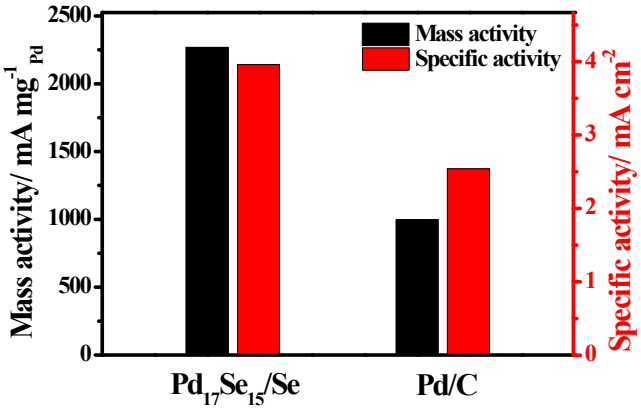

Fig. S8 Graphical comparison of mass and specific activity of $Pd_{17}Se_{15}$/Se and Pd/C catalysts for ethanol oxidation in the 1 M KOH + 1 M CH_3CH_2OH.

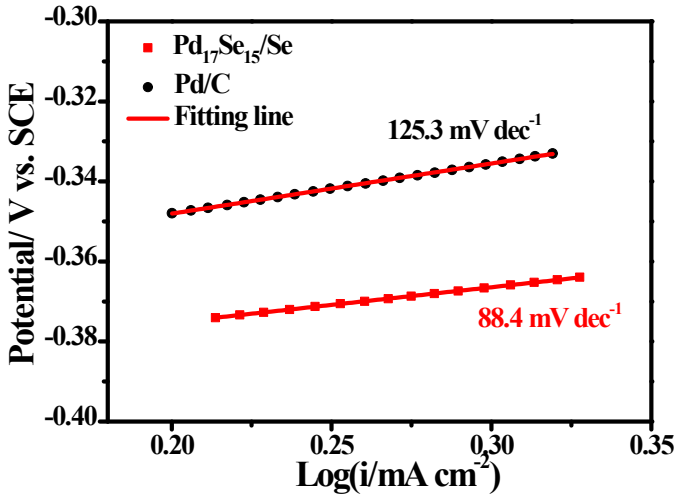

Fig. S9 Tafel plots of $Pd_{17}Se_{15}$/Se and Pd/C catalysts for ethanol oxidation.

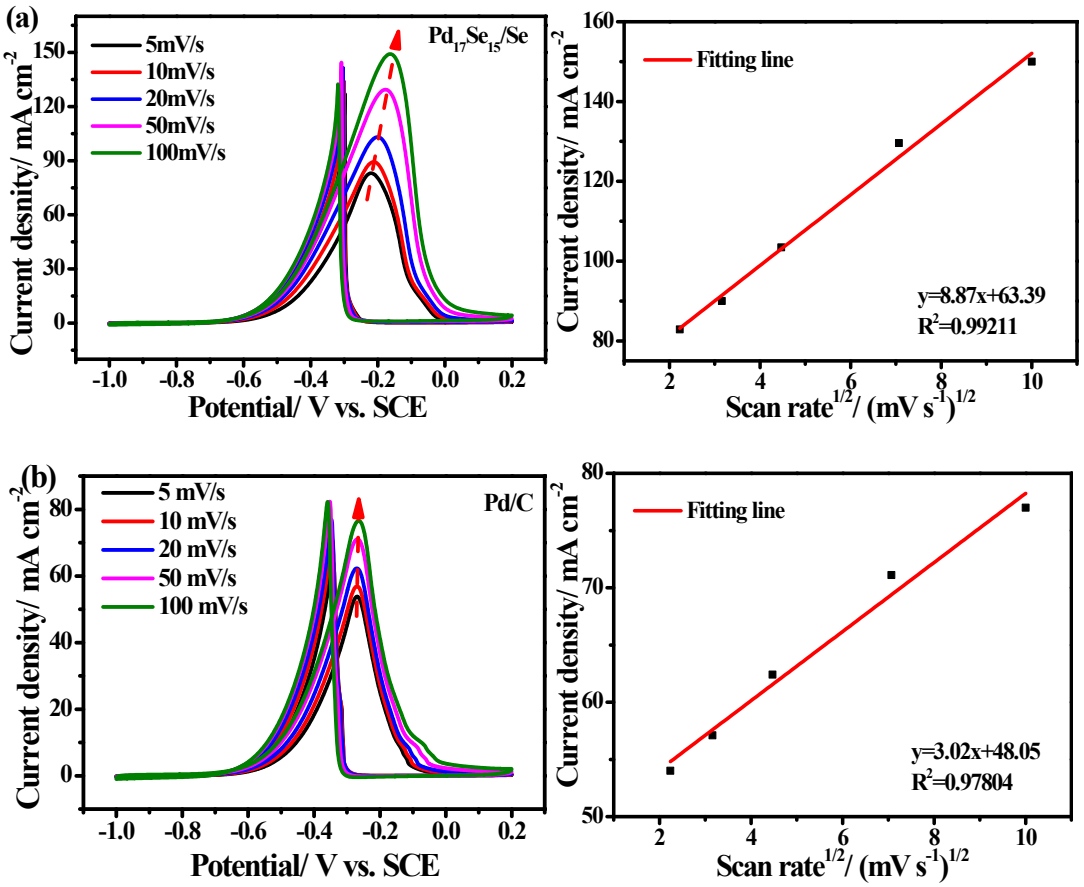

Fig. S10 Cyclic voltammograms of the $Pd_{17}Se_{15}$/Se (a) and Pd/C (b) catalysts in 1 M KOH + 1 M CH_3CH_2OH at scan rates of 5, 10, 20, 50, 100 mV s^{-1} and the corresponding peak current density versus the square root of the scan rates.

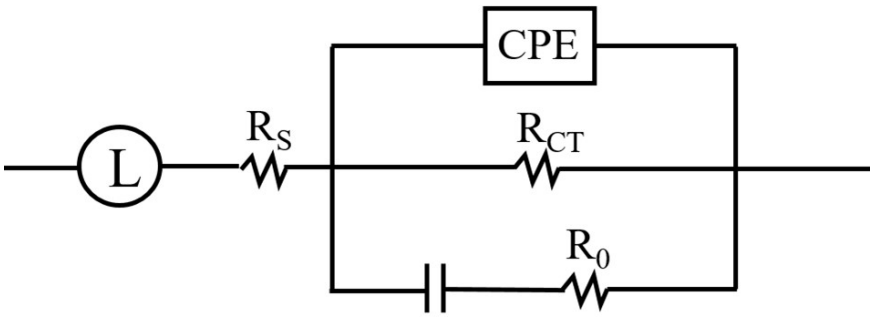

Fig. S11 Equivalent circuit for EIS analysis in the 1 M KOH + 1 M CH_3CH_2OH solution.

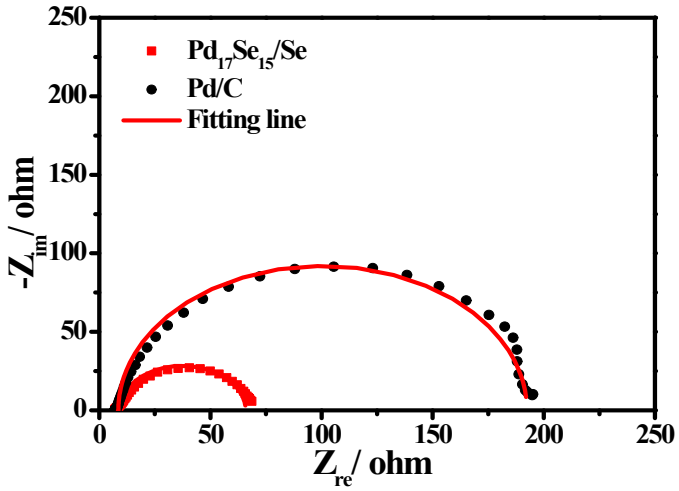

Fig. S12 Nyquist plots of $Pd_{17}Se_{15}$/Se and Pd/C catalysts for ethanol oxidation.

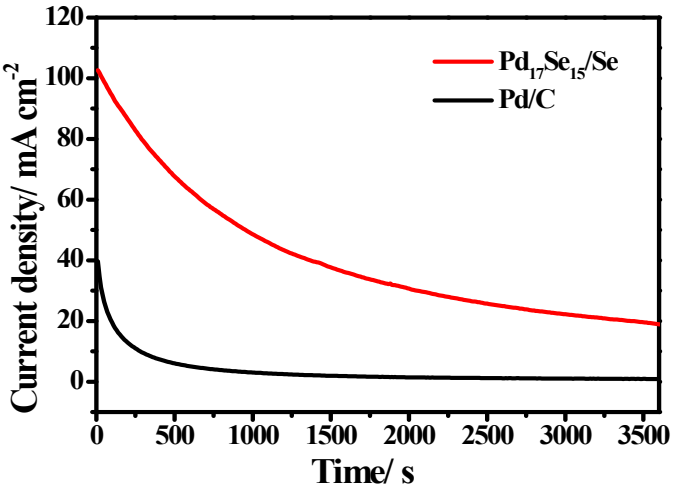

Fig. S13 Chronoamperometry curves recorded at -0.25 V for ethanol oxidation during 3600 s.

Table S1 The energy-dispersive X-ray spectroscopy (EDX) composition of $Pd_{17}Se_{15}$/Se catalyst.

Element	Weight %	Atomic %
C	2.05	13.24
Se	59.01	58.23
Pd	38.94	28.53

Table S2 Binding energy of Pd $3d_{5/2}$ and $3d_{3/2}$ components for $Pd_{17}Se_{15}$/Se and Pd/C catalysts.

Catalysts	3d 5/2		3d 3/2		Content (Pd^{2+}) / %
	Peak	Binding energy/eV	Peak	Binding energy/eV	
Pd/C	Pd^0	335.4	Pd^0	340.6	27.8
	Pd^{2+}	336.4	Pd^{2+}	341.6	
$Pd_{17}Se_{15}$/Se	Pd^0	335.7	Pd^0	340.9	32.1
	Pd^{2+}	336.7	Pd^{2+}	341.9	

Table S3 Mulliken atomic population analysis of the Pd in $Pd_{17}Se_{15}$.

Ion	s	p	d	Total	Charge (e)
1	2.54	6.12	8.72	17.38	0.62
2	2.53	6.15	8.81	17.49	0.51
3	2.54	6.12	8.72	17.38	0.62
4	2.66	6.11	8.69	17.46	0.54
5	2.83	6.21	8.66	17.70	0.30
6	2.66	6.11	8.69	17.46	0.54
7	2.66	6.11	8.69	17.46	0.54
8	2.84	6.22	8.63	17.69	0.31
9	2.66	6.11	8.69	17.46	0.54
10	2.54	6.12	8.72	17.38	0.62
11	2.53	6.15	8.81	17.49	0.51
12	2.54	6.12	8.72	17.38	0.62
13	2.66	6.11	8.69	17.46	0.54
14	2.83	6.21	8.66	17.70	0.30
15	2.66	6.11	8.69	17.46	0.54
16	2.54	6.12	8.72	17.38	0.62
17	2.53	6.15	8.81	17.49	0.51
The average charge					0.52

Table S4 Comparisons of activities of some Pd-based catalysts reported in the 1 M KOH + 1 M CH_3OH solution.

Catalysts	Mass activity/mA mg^{-1}_{Pd}	Reference
Pd-Au (1 : 1)/RGO	1218.4	[4]
Pd-PdO PNTs-260	1111.3	[5]
NP-PdAu	866.5	[6]
Pd modified Ni nanowire	900	[7]
Pd/NCNTs@NGS	1046	[8]
Pd_2Cu_2/rGO	916	[9]
PdCu-5 nanocages	1090	[10]
PdCu/VrGO	760	[11]
Pd NPs/Ni-Eth	1021.96	[12]
$Pd_{30}Au_{70}$/C	950.6	[13]
Pd-PdO PNTs-260	1111.3	[14]
$Pd_{72}Cu_{14}Co_{14}$/rGO	1062	[15]
Pd-$Ti_3C_2T_x$ MXene	390	[16]
Pd_3Rh_1	440	[17]
5% PdAu NW	1021.4	[18]
$Pd_{17}Se_{15}$/Se	1321.3	This work
Pd/C	417.2	This work

Note: The reported performance might be influenced by the different test procedure, but the trend can be obtained.

Table S5 EIS fitting parameters from equivalent circuits for different catalysts in the 1 M KOH +1 M CH_3OH solution.

Catalysts	**R_s/ Ω**	**CPE/ S**	**R_{ct}/ Ω**	**L/ H**	**R_0/ Ω**
Pd/C	8.68	2.662×10^{-4}	262.1	69.76	17.4
$Pd_{17}Se_{15}$/Se	7.11	2.646×10^{-4}	141	65.1	73.34

Table S6 Comparisons of activities of various Pd-based catalysts reported in the 1 M KOH + 1 M CH_3CH_2OH solution.

Catalysts	Mass activity/mA mg^{-1}_{Pd}	Reference
Pd modified Ni nanowire	1479.79	[7]
Pd/CNTA	1484.4	[19]
Pd/BN-GNRs	2156	[20]
$Pd/Ni(OH)_2/rGO$	1546	[21]
Pd_3Y/GNS	1780	[22]
Pd/NCB@NGS-1	1919.5	[23]
Pd @CoP NSs/CFC	1413	[24]
Pd/NCNTs@NGS	1823	[25]
Pd-Au BHTs	2124	[26]
PdCo NTAs/CFC	1562	[27]
PdBP MSs	1450	[28]
$Pd/Ni(OH)_2/rGO$	1550	[29]
PdAg NSAs	1870	[30]
$Pd\text{-}PdO_x/GS\text{-}NH_2$	1319.9	[31]
$Pd\text{-}WO_{2.75}NB$	1980	[32]
$Pd_{17}Se_{15}/Se$	2268	This work
Pd/C	998.2	This work

Table S7 EIS fitting parameters from equivalent circuits for different catalysts in the 1 M KOH +1 M CH_3CH_2OH solution.

Catalysts	L/H	R_s/Ω	CPE /S	R_{ct}/Ω	R_0/Ω
Pd/C	1.025×10^{-5}	8.97	8.6×10^{-8}	192.3	1.00×10^{-2}
$Pd_{17}Se_{15}$/Se	1.598×10^{-5}	8.79	2.0×10^{-7}	65.8	6.60×10^{-8}

References

1. Q. Tan, C. Shu, J. Abbott, Q. Zhao, L. Liu, T. Qu, Y. Chen, H. Zhu, Y. Liu and G. Wu, *ACS Catal.*, 2019, **9**, 6362-6371.
2. Z. Yu, S. Xu, Y. Feng, C. Yang, Q. Yao, Q. Shao, Y.-f. Li and X. Huang, *Nano Lett.*, 2021, **21**, 3805-3812.
3. X. Cao, X. Zhao, J. Hu and Z. Chen, *Phys. Chem. Chem. Phys.*, 2020, **22**, 2449-2456.
4. F. Li, Y. Guo, R. Li, F. Wu, Y. Liu, X. Sun, C. Li, W. Wang and J. Gao, *J. Mater. Chem. A*, 2013, **1**, 6579-6587.
5. T. Wang, F. Li, H. Huang, S. Yin, P. Chen, P. Jin and Y. Chen, *Adv. Funct. Mater.*, 2020, **30**, 2000534.
6. X. Wang, B. Tang, X. Huang, Y. Ma and Z. Zhang, *J. Alloy. Compd.*, 2013, **565**, 120-126.
7. R. Kottayintavida and N. K. Gopalan, *Int. J. Hydrog. Energy*, 2020, **45**, 8396-8404.
8. S. Li, H. Yang, H. Zou, M. Yang, X. Liu, J. Jin and J. Ma, *J. Mater. Chem. A*, 2018, **6**, 14717-14724.
9. H. Ye, Y. Li, J. Chen, J. Sheng, X. Fu, R. Sun and C. Wong, *J. Mater. Sci.*, 2018, **53**, 15871-15881.
10. J. Sheng, J. Kang, H. Ye, J. Xie, B. Zhao, X. Fu, Y. Yu, R. Sun and C. Wong, *J. Mater. Chem. A*, 2018, **6**, 3906-3912.
11. L. Yang, D. Yan, C. Liu, H. Song, Y. Tang, S. Luo and M. Liu, *J. Power. Sources*, 2015, **278**, 725-732.
12. H. Lei, X. Li, C. Sun, J. Zeng, S. S. Siwal and Q. Zhang, *Small*, 2019, **15**, 1804722.
13. Z. Yin, M. Chi, Q. Zhu, D. Ma, J. Sun and X. Bao, *J. Mater. Chem. A*, 2013, **1**, 9157-9163.
14. T.-J. Wang, F.-M. Li, H. Huang, S.-W. Yin, P. Chen, P.-J. Jin and Y. Chen, *Adv. Funct. Mater.*, 2020, **30**, 2000534.
15. F. Yang, B. Zhang, S. Dong, C. Wang, A. Feng, X. Fan and Y. Li, *J. Energy Chem.*, 2019, **29**, 72-78.
16. Z. Lang, Z. Zhuang, S. Li, L. Xia, Y. Zhao, Y. Zhao, C. Han and L. Zhou, *ACS Appl. Mater. Interfaces*, 2020, **12**, 2400-2406.
17. Q.-Y. Hu, R.-H. Zhang, D. Chen, Y.-F. Guo, W. Zhan, L.-M. Luo and X.-W. Zhou, *Int. J. Hydrog. Energy*, 2019, **44**, 16287-16296.
18. R. Kottayintavida and N. K. Gopalan, *Electrochim. Acta*, 2021, **384**, 138405.
19. F. Hu, X. Cui and W. Chen, *J. Phys. Chem. C*, 2010, **114**, 20284-20289.
20. Q. Liu, J. Fan, Y. Min, T. Wu, Y. Lin and Q. Xu, *J. Mater. Chem. A*, 2016, **4**, 4929-4933.
21. W. Huang, X.-Y. Ma, H. Wang, R. Feng, J. Zhou, P. N. Duchesne, P. Zhang, F. Chen, N. Han, F. Zhao, J. Zhou, W. Cai and Y. Li, *Adv. Mater.*, 2017, **29**, 1703057.
22. M. Seo, S. Choi, J. Seo, S. Noh, W. Kim and B. Han, *Appl. Catal. B.*, 2013, **129**, 163-171.
23. S. Li, J. Shu, S. Ma, H. Yang, J. Jin, X. Zhang and R. Jin, *Appl. Catal. B: Environ.*, 2021, **280**, 119464.
24. S. Ye, J. Feng and G. Li, *ACS Catal.*, 2016, **6**, 7962-7969.
25. S. W. Li, H. L. Yang, H. Zou, M. Yang, X. D. Liu, J. Jin and J. T. Ma, *J. Mater. Chem. A*, 2018, **6**, 14717-14724.

26. C. Cui, J. Yu, H. Li, M. Gao, H. Liang and S. Yu, *ACS Nano*, 2011, **5**, 4211-4218.
27. A. Wang, X. He, X. Lu, H. Xu, Y. Tong and G. Li, *Angew. Chem. Int. Edit.*, 2015, **54**, 3669-3673.
28. H. Lv, D. Xu, L. Sun, J. Henzie, S. L. Suib, Y. Yamauchi and B. Liu, *ACS Nano*, 2019, **13**, 12052-12061.
29. W. Huang, X.-Y. Ma, H. Wang, R. Feng, J. Zhou, P. N. Duchesne, P. Zhang, F. Chen, N. Han, F. Zhao, J. Zhou, W.-B. Cai and Y. Li, *Adv. Mater.*, 2017, **29**, 1703057.
30. M. Yang, X. Lao, J. Sun, N. Ma, S. Wang, W. Ye and P. Guo, *Langmuir*, 2020, **36**, 11094-11101.
31. H. Yang, S. Li, F. Feng, S. Ou, F. Li, M. Yang, K. Qian, J. Jin and J. Ma, *ACS Sustain. Chem. Eng.*, 2019, **7**, 14621-14628.
32. L. Karuppasamy, C.-Y. Chen, S. Anandan and J. J. Wu, *ACS Appl. Mater. Interfaces*, 2019, **11**, 10028-10041.